Special Issue for ICASGE'19

Bearing Capacity Evaluation under Gravity Walls

Hassan Abouseeda and Ahmed Fouad

Bearing Capacity Evaluation under Gravity Walls

Hassan Abouseeda[1] and Ahmed Fouad[2]

[1] *Associated professor, Faculty of Engineering, Alexandria University, Egypt*
E-mail: hassan@geotechegypt.com
[2] *Teaching Assistant, Faculty of Engineering, Alexandria University, Egypt*
E-mail: ahmedfouad927@gmail.com

ABSTRACT

This paper presents a new limit equilibrium (LE) approach for evaluating the ultimate bearing capacity of strip shallow foundations with different embedment heights resting on sandy soil and based on Meyerhof assumptions. Then presented LE approach has been used to evaluate bearing capacity for gravity walls with varied embedment height to width ratios (h/B). In order to facilitate the calculations, new stress distribution equations have been integrated for semi-infinite uniform strip load using Boussinesq solution. Governing parameters have been examined individually to determine their effects on the ultimate bearing capacity, such as live load, foundation and wall backfilling soil friction angles, and h/B. Finite element analyses (FEA) with Mohr-Coulomb material model has been used to verify and calibrate the proposed LE calculations. Calculated bearing capacity - for foundation soil with different embedment heights on each side averaged along foundation width – has been related to bearing capacity of similar foundation with lowest embedment height value as improvement factor (I_f). Due to unevenness of embedment, soil wall contact stresses at failure become uneven. Partial shear failure factor (PSFF) is produced to represent its shear failure surface which developed in soil at the side with higher embedment. Comparing I_f which calculated from the proposed approach to FEA results, PSFF ranged between 0.522 and 0.255 for live load to width ratios (LL/B) from 0.0 to 10.0 and ranged between 0.675 and 0.411 for h/B from 0.5 to 2 at soil friction angle 30°, 33°, 36°. PSFF diversify is inversely proportional to h/B and LL/B. I_f ranged from 1 for equal side embedment to 2.866 as maximum for unequal side embedment. I_f diversity is proportional to h/B and soil friction angle.

Keywords: *Gravity wall, Bearing capacity, Cohesionless Soil, Soil failure mechanism, Limit equilibrium method, MATLAB, Finite element method.*

INTRODUCTION

Gravity walls have been widely used for enormous projects such as roads, tunnels and mainly in marines. Although ultimate bearing capacity of soil under different shallow foundations has extensive studies and theories, researches seldom studied it beneath gravity wall with varied embedment heights. Ultimate bearing capacity and shear strength parameters are difficult processes to be evaluated. Historically, bearing capacity design considerations have combined minimizing potential shear failure of soil and limiting vertical settlement which both are a function of the footing width and excluding varied embedment height effect.

Generally, footings – on isotropic homogenous soil without embedment - with higher width (*B*) increases safety factor, but the stress increase is more deeply extended below bearing depth.

Table 1 List of symbols

B	Footing Width	*D*	depth of embedment
b	Half Footing Width	θ	logarithmic spiral angle
q_u	Ultimate Bearing Capacity	r	Radius of logarithmic spiral
c	Cohesion	r_o	Initial Radius of logarithmic spiral

N_c, N_q, λ_q	Bearing Capacity Factors	Fh	Driving force
γ	Unit Weight	fh	Horizontal stress
$\lambda_{cs}, \lambda_{qs}, \lambda_{\gamma s}$	Shape Factors	Fv	Vertical stress
$\lambda_{cd}, \lambda_{qd}, \lambda_{\gamma d}$	Depth Factors	W	Soil weight
ϕ	Friction angle	fr, fl	embedment left and right stress increase
σ_{xx}, σ_{zz}	Principal Stresses	Kp	Passive earth pressure
τ	Shear Strength	Fr	Resistance force
$\Delta\sigma z$,	Vertical Stress Increase	E	Young's Modulus
$\Delta\sigma x$	Horizontal Stress Increase	ν	Poisson's ratio
b	Half footing Width	ψ	Dilation angle
x, y, z	Cartesian Coordinates	Q	Average contact stress
q	Surcharge load	Q_o	Bearing capacity for lower embedment side

Three failure mechanisms, which result from stresses exceed soil ultimate bearing capacity, are general, local and punching shear failures [1].

The bearing capacity of a shallow strip footing is commonly determined by using Terzaghi equation for Strip foundation [2].

$$q_u = cN_c + qN_q + 0.5\gamma BN_\gamma \qquad\qquad 1$$

Meyerhof [3] published a theory that could be applied to rough, shallow and deep foundation. He considered a shape factor with the depth, the effect of shear resistance along the failure surface in the soil situated above the foundation (depth factors) and inclination factors during inclined loading that Terzaghi neglected. Meyerhof suggested a generalized method to estimate the ultimate bearing capacity for centrally vertically loaded foundation as.

$$q_u = cN_c\lambda_{cs}\lambda_{cd} + qN_q\lambda_{qs}\lambda_{qd} + 0.5\gamma BN_\gamma\lambda_{\gamma s}\lambda_{\gamma d} \qquad\qquad 2$$

Several terms should be considered in order to precisely evaluate the ultimate bearing capacity under gravity wall, such as embedment height to bearing width ratio (h/B), backfill friction angle and live load, which are mathematically modeled as novel limit equilibrium approach (LEA) and solved using MATLAB. Additionally, new stress distribution equations are integrated for semi-infinite uniform strip load using Boussinesq solution to facilitate the calculation process.

In recent years, Finite Element Analysis (FEA) has been widely used in geotechnical studies to investigate soil behavior [4, 5]. Bearing capacity analysis using FEA are commonly used to simplify computations and save the time of experimental analysis. Therefore, several computer programs based on FEA have been receiving much attention over recent decades as powerful tools for solving complex cases.

This approach demonstrates how to apply FEA to evaluate bearing capacity of gravity wall on a sandy soil using the explicit finite element software "Midas GTSNX 2019 v1.1".

This research has used Mohr-Coulomb (MC) material model to verify and calibrate the proposed LEA calculations. MC failure criterion is a set of linear equations in principal stress space, using plain strain consideration in MC which can be written as:

$$(\sigma_{xx} - \sigma_{zz}) = (\sigma_{xx} + \sigma_{zz})\,\text{Sin}\,\phi + 2c\,\text{Cos}\,\phi \qquad\qquad 3$$

Where Major σ_{xx} and minor σ_{zz} principal stresses (σ_{yy} is neglected).

It can be also written as normal stress σ and shear stress τ on the failure plane [6].

$$\tau = c + \alpha \tan\phi \qquad\qquad 4$$

Mohr's condition is based on the assumption that failure depends on σ_{xx} and σ_{zz} only; the shape of the failure envelope and the loci of σ, τ acting on a failure plane can be linear or nonlinear [7] . Coulomb's condition is based on a linear failure envelope to determine the critical combination of σ, τ that will cause failure on the same plane [8]. A linear failure criterion with an intermediate stress (σ_{yy}) effect was described by Paul [9] and implemented by Meyer JP [10].

Governing parameters have been examined individually in order to determine their effects on the ultimate bearing capacity, such as live load behind the wall, foundation and backfilling friction angle, and depth to width ratio (h/B).

Methodology

Firstly, in order to facilitate the novel limit equilibrium approach (LEA), this study has integrated semi-infinite surface strip equation as shown in equation (7). Secondly, a mathematical study has used LEA to evaluate driving and resistance stresses on soil shear failure surface developed under shallow foundations to balance the overall stability and validate the results with Meyerhof equation. Finally, the same approach was used to balance the overall stability under gravity wall which was calibrated and validated by Midas GTSNX 2019 v1.1 software.

**Stresses in Soil Mass Due to Semi-Infinite Strip Load**

Boussinesq [11] solved the problem of stresses produced at any point in a homogeneous, elastic, and isotropic soil for line load of infinite length inside the soil mass using the theory of elasticity principles, or

$$\Delta\sigma_z = \frac{2qz^3}{\pi(r^2+z^2)^2} \qquad\qquad 5$$

This study has integrated line load equation of Boussinesq in uniform x direction to infinite distance to get the vertical stress due to infinite surface strip stress $\Delta\sigma_z$ represented in equation (6) and shown in Figure (1-A). The Vertical stress distribution is as following:

$$\Delta\sigma_z = \int_{-b}^{10000000} \frac{2qz^3}{\pi(x^2+z^2)^2}\,dx \qquad\qquad 6$$

$$\Delta\sigma_z = \frac{2(\gamma h)z^3\left(\frac{1000000z+(1000000000000+z^2)ArcTan[\frac{1000000}{z}]}{2z^3(1000000000000+z^2)}+\frac{(b+x)z+(b^2+2bx+x^2+z^2)ArcTan[\frac{b+x}{z}]}{2z^3(b^2+2bx+x^2+z^2)}\right)}{\pi} \qquad 7$$

(A)   (B)   (C)
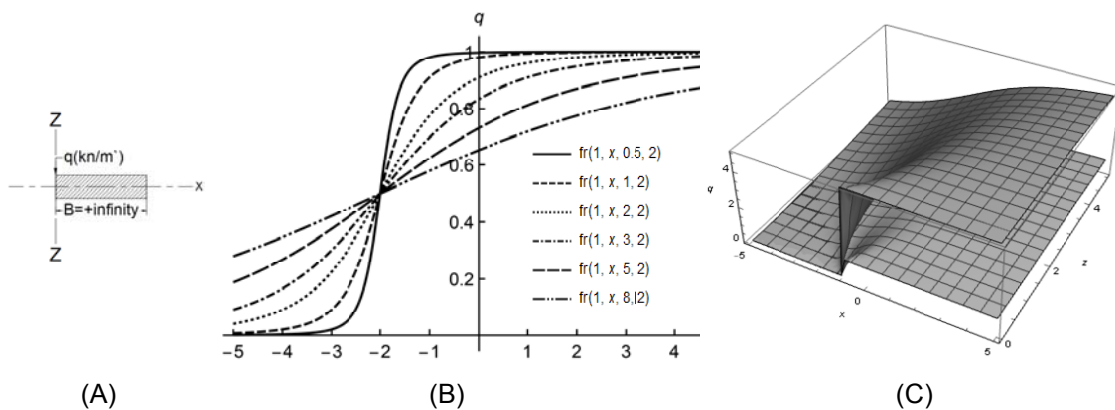
Figure (1) A- Semi-infinite load on soil, B- Vertical stress distribution $\Delta\sigma_v$=fr (q, x, z, b) C- 3D Vertical stress distribution

Ultimate Bearing Capacity Evaluation for Shallow Foundation

Meyerhof [3] used Prandtl [12] wedges and set his assumptions to draw the shear failure surface in the soil. Prandtl divided the shear failure surface into three zones, in which the first

wedge (elastic zone1) is an equilateral triangle with angle $45^o+0.5\phi^o$ under the shallow foundation. The second wedge is a logarithmic spiral of $r=r_o^{\theta tan(\phi)}$ (zone 2) which transfers stresses to the third zone. Finally, the third is an equilateral triangle with angle $45^o-0.5\phi^o$, which called the Rankine passive wedge (Zone 3), and moves towards the ground surface. Meyerhof assumptions are based on (a) the plane of failure is symmetric around the center line of shallow foundations (Figure (2-A)), (b) the contact stress below the foundation is uniform (Figure (2-B)). Meyerhof assumptions and developed shear failure surface have been used to study and calculate driving forces under shallow foundations.
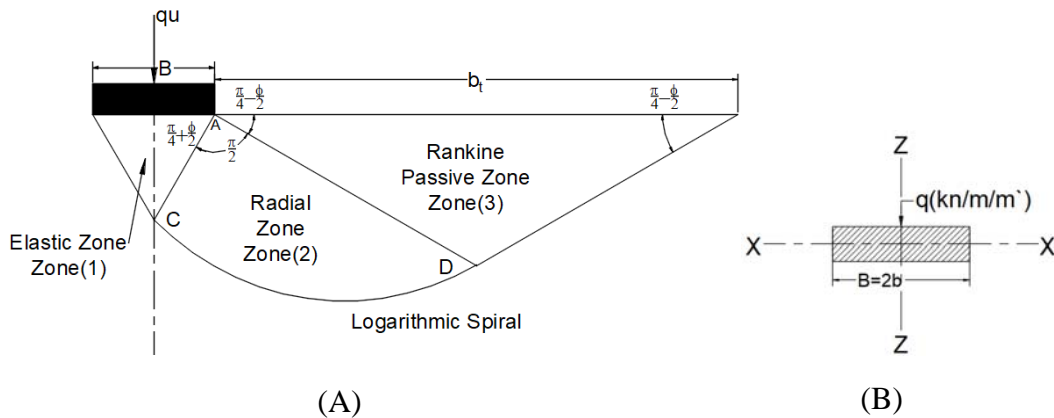

(A)   (B)

Figure (2) A- Symmetric shear failure surface of Meyerhof theory (1951)
B- Contact stress distribution below the foundation

Developed Deriving Stresses

Foundation weight and loads are transferred vertically and horizontally through soil domain which force the failure wedge (ACDB) to upheave whenever foundation contact stresses exceed the soil bearing capacity. ACDB has been divided to multi segments and horizontal stresses have been calculated at its ends to be integrated and get the total driving force (Figure (3)). Then study used the calculated driving force (Fh) to be compared with resistance force in equations (8-12).
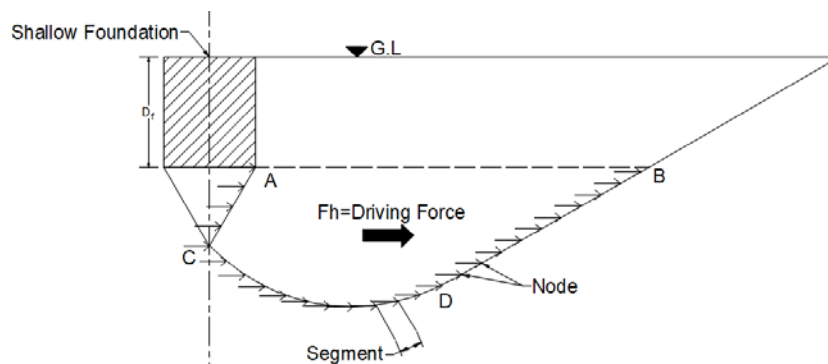

Figure (3) Deriving stress distribution over shear failure surface

Developed Resistance Stresses

However horizontal stresses (fh) developed on soil shear failure surface due to contact stress drive the ACDB zone to upheave, the vertical component (fv), the stresses due to two sides embedment (fl, fr) and soil weight (w) resist the shear failure.

Vertical stresses distribution due to embedment height has been calculated by the novel integrated equation (7). Rankine passive zone resist to soil stresses horizontally by Rankine passive coefficient (K_p) due to all vertical stresses (fv, w, fl, fr) component (Figure (4)). Meyerhof soil shear failure surface with resistance stresses and integrated resistance forces are presented in equations (8-12).

- Horizontal stress developed on the plan of failure

$$fh = (fr + fl)K_p \qquad\qquad 8$$

$$K_p = \frac{1+\sin\phi}{1-\sin\phi} \qquad\qquad 9$$

$$Fn = (fv + w + fr + fl)\cos\varepsilon + fh\sin\varepsilon$$

- Shear force at the segment

$$\tau = Fn\tan\phi$$

$$\qquad\qquad 10$$

- Horizontal resistance force

$$fr = \tau\cos\varepsilon = (fv + w)\cos\varepsilon\,\tan\phi \qquad\qquad 11$$

$$\sum Fr = \sum_0^n fr$$
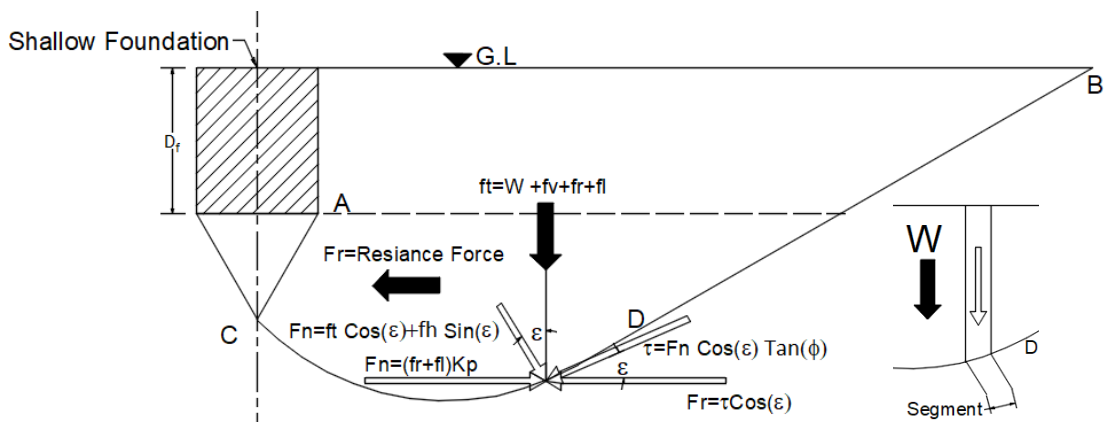
Error! Bookmark not defined.

Figure (4) Horizontal resistance force calculation on shear failure surface

Overall Forces Equilibrium

Equilibrium analysis between driving and resistance forces has been examined. Then the approached is solved using MATLAB to get accurate results of the bearing capacity under foundations.

Validation process has been implemented using Meyerhof equation by changing embedment heights from 0 to 10 m for soil friction angle 30° and foundation width 4.0 m, and the results exhibited adequate agreement as shown in Table **2**. Figure (5) compares Meyerhof equation to the novel LEA with maximum error 2.68 %.

Table 2 Comparison between Meyerhof equation result and the novel limit equilibrium approach results

Embedment depth (m)	LEA (kN/m^2)	Meyerhof (kN/m^2)	Difference (kN/m^2)	Error (%)
0	544	532	-8	-1.50
1	882	882	-1	-0.11
2	1242	1258	16	1.27
3	1622	1662	39	2.35
4	2036	2093	56	2.68
5	2495	2550	55	2.16
6	2988	3035	47	1.55
7	3492	3546	55	1.55
8	4033	4086	53	1.30
9	4616	4652	36	0.77
10	5242	5246	3	0.06
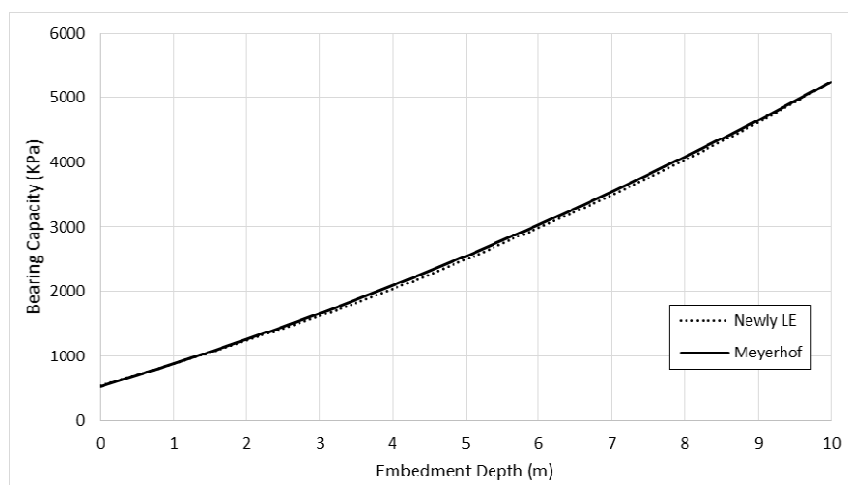
Figure (5) Bearing capacity Comparison between Novel limit equilibrium approach and Meyerhof equation[3]

Bearing Capacity for gravity walls

The same approach which has been coded, calibrated and validated for shallow foundations has been used to calculate bearing capacity under gravity walls except loading criteria (Figure (6)) and unsymmetrically shear failure surface as shown in Figure (7) and Figure (8).

Loading criteria for bearing capacity under gravity walls has been calculated by two inverted triangles and merging their effect to examine the increase of the averaged contact stress (Q) to the bearing capacity according to the lower embedment height side (Q_o) (Figure (6)).
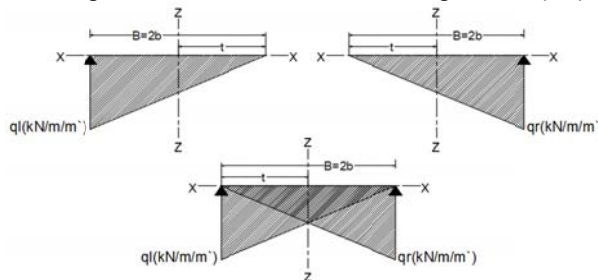

Figure (6) contact triangular stress distribution under the gravity wall

Figure (7) illustrates developed driving stresses due to differential embedment height under gravity walls.

Figure (8) and equations (16-29) show soil resistance stresses under gravity walls and the mathematical calculations to obtain the resistance force. The additional force (F_{add}) due to differential embedment height has been integrated from its stresses $\Delta\sigma_{add}$ using equation (15).

The driving and the resistance force are calculated then the contact stress (qr, ql) under the shallow foundation keeps changing until both horizontal forces maintain Equilibrium. This equilibrium has been examined by the MATLAB code. Additionally, bearing capacity under gravity walls was calculated as the average between right and left contact end stresses (*qr*, *ql*).

Due to unevenness of embedment, soil wall contact stresses at failure become uneven. Despite the fully shear failure surface generated at the lower embedment side, partial shear failure surface is developed at the other side due to differential resistance force (Figure (9)).
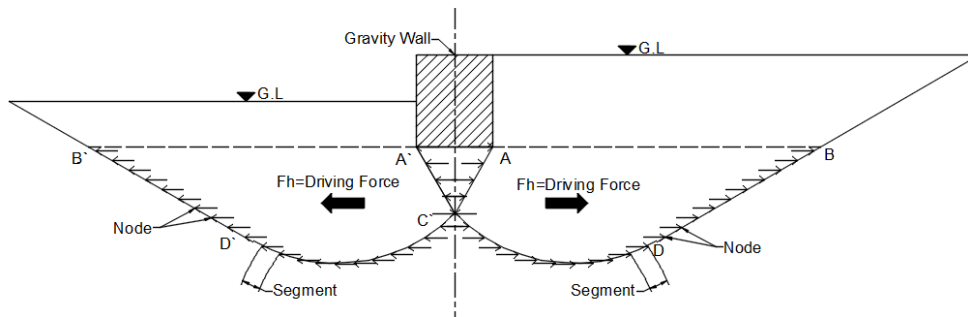

Figure (7) Deriving stress distribution

$$\Delta\sigma_x = \frac{2qzx^2}{\pi(x^2+z^2)^2} \tag{12}$$

Where $q = \gamma \, x \, \Delta h_{add}$

$$\Delta\sigma_x = \int_b^{bs} \frac{2qtzx^2}{2\pi b(x^2+z^2)^2} dt \tag{13}$$

$$\Delta\sigma_{add} = \frac{2qz^3\left(\frac{bcz+(bc^2+z^2)ArcTan[\frac{bc}{z}]}{2z^3(bc^2+z^2)} - \frac{(-b+x)z+2bxArcTan[\frac{b-x}{z}]+(b^2+x^2+z^2)ArcTan[\frac{-b+x}{z}]}{2z^3(b^2-2bx+x^2+z^2)}\right)}{\pi} \tag{14}$$

<u>The right shear failure surface</u>

- $$K_p = \frac{1+\sin\phi}{1-\sin\phi} \tag{15}$$

- Horizontal stress developed on the plan of failure

$$fh = (fr + fl)K_p \tag{16}$$

- Horizontal stress developed on the plan of failure

$$F_{add}^` = F_{add}\cos\varepsilon + (F_{add}xK_p)\sin\varepsilon \tag{17}$$

$$F_{add}^` = F_{add}\cos\varepsilon + (F_{add}xK_p)\sin\varepsilon$$

$$Fn = (fv + w + fr + fl)\cos\varepsilon + fh\sin\varepsilon \tag{18}$$

- Shear force at the segment

$$\tau = (Fn + F_{add}^`)\tan\phi \tag{19}$$

- Horizontal resistance force

$$fr = \tau\cos\varepsilon \tag{20}$$
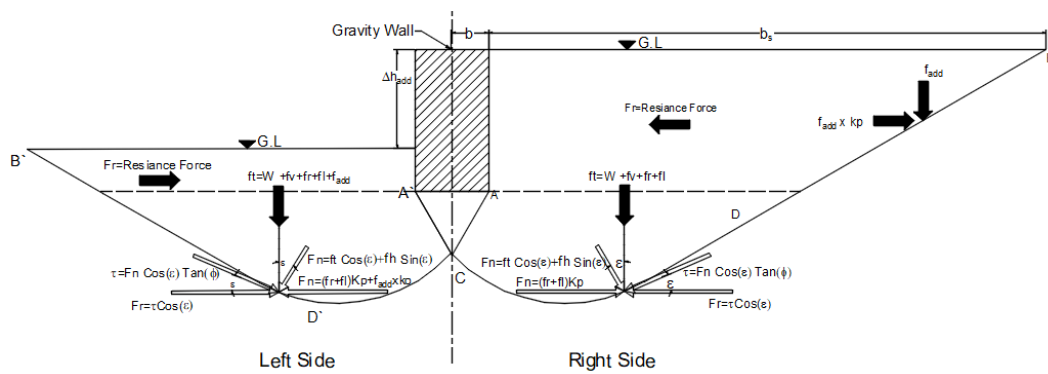
$$\sum Fr = \sum_0^n fr \tag{21}$$

<u>For the left shear failure surface</u>

- Horizontal stress developed on the plan of failure

$$fh` = (fr` + fl`)K_p \qquad 22$$

- Horizontal stress developed on the plan of failure

$$F_{add}^{``} = F_{add} K_o \qquad 23$$

$$K_o = 1 - \sin \phi \qquad 24$$

$$Fn = (fv` + w + fr` + fl` + F_{add}) \cos \varepsilon + (fh + F_{add}^{``}) \sin \varepsilon \qquad 25$$

- Shear force at the segment

$$\tau = Fn \tan \phi \qquad 26$$

- Horizontal resistance force

$$fr = \tau \cos \varepsilon \qquad 27$$

$$\sum Fr = \sum_0^n fr \qquad 28$$

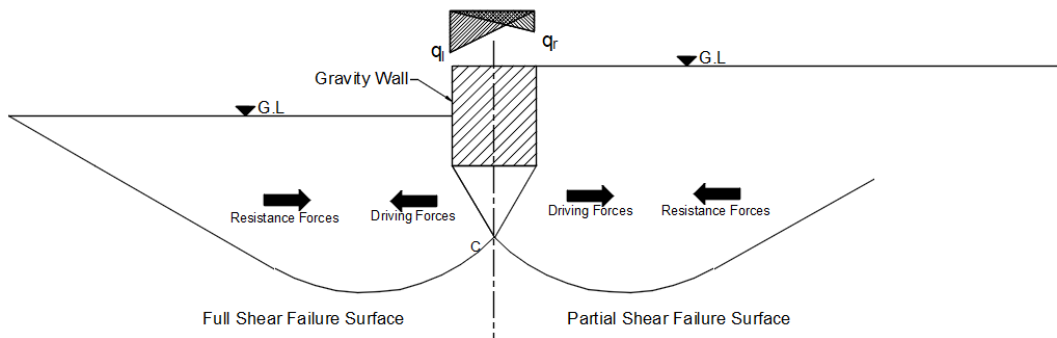**Figure (8) Horizontal resistance force calculation**

Figure (9) over all forces Equilibrium

Results

After analysis for the novel limit equilibrium approach (LEA) using MATLAB code and finite element analysis (FEA) models in addition to calibration and validation processes, over fifty models were created to discuss the interrelationships of improvement factor under gravity wall ($I_f=Q/Q_o$), the partial shear failure factor (PSFF), embedment height to bearing width ratio (h/B), soil friction angle, wall width (B) and live load to width ratio (LL/B) as can be shown from figures (10-13).

Finite Element Analysis (FEA) Under Gravity Walls

Building finite element models based on Mohr –Coulomb material for different soil friction angles, soil young's modulus and poisson's ratio (Table 3) were compared with the novel LEA under gravity walls to calculate contact averaged bearing capacity (Q). There is no difference between any of the load or the displacement controlled. However, as the displacement could be increased without increasing the loads, the displacement controlled was chosen in this analysis since it can reach higher settlement values. Figure (10) shows sample of numerically finite element models.

The finite element results in Figure (10) were compared to the novel LEA (Figure (8)) in Table 4.

Table 3 Material properties of sandy soil – Mohr-Coulomb

Parameter	Soil 1	Soil 2	Soil 3
Unit weight γ (kN/m^3)	17.0	17.0	17.0
Angle of friction ϕ^o	30	33	36
Young's Modulus E (kN/m^2)	20000	30000	40000
Poisson's ratio v	0.33	0.31	0.29
Dilation angle ψ^ρ	0	3	6
Interface reduction factor	0.67	0.67	0.67

Table 4 Comparing between results of the novel limit equilibrium approach and Finite Element Analysis

Parameter	Value	Parameter	Value
Friction angle (Deg)	30	ql-LE (kN/m^2)	3231.00
Wall Width B (m)	8	qr-LE (kN/m^2)	1947.80
h/B	1.5	Average stress Q-LE (kN/m^2)	2589.40
Live Load LL (kN/m^2)	40	ql (FEA) (kN/m^2)	2908.00
Improvement factor (I_f=Q/Q$_o$)	2.21	qr (FEA) (kN/m^2)	2341.60
PSFF	0.3960	Average stress (FEA) (kN/m^2)	2624.80
Error (%)	1.37		
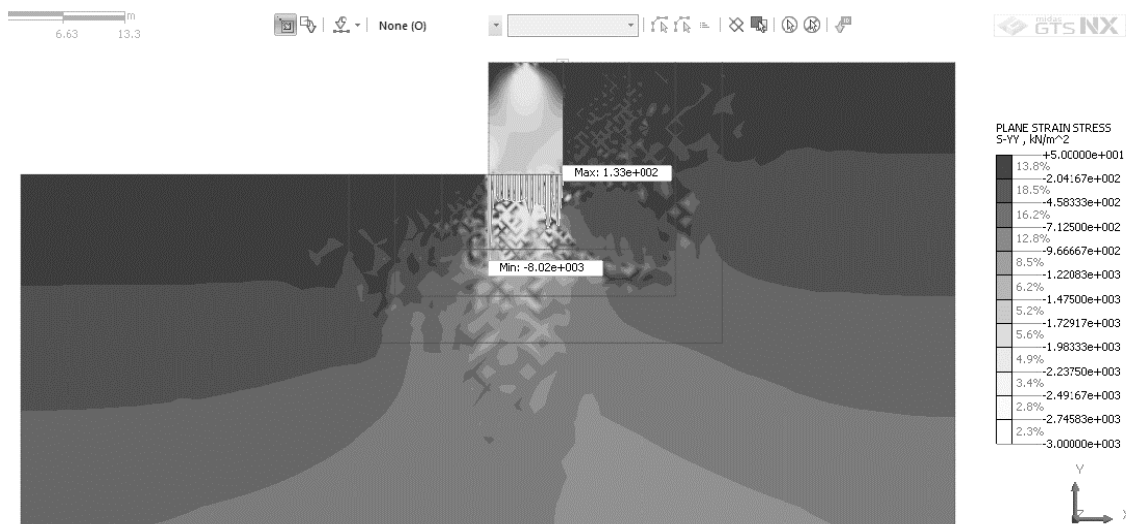
Figure (10) Finite element model for gravity wall of with 8.0 m, LL/B=5.0 and soil angle of friction 30° with h/B=1.5

The improvement factor (I_f) is obtained from the ratio between averaged contact stress (Q) to bearing capacity stress under gravity walls measured at lower embedment side (Q$_o$).

Improvement factor (I_f) refers to the increase of bearing capacity due to differential embedment height.

Comparison between the novel LEA and FEA to get the improvement factor ($I_f = Q/Q_o$) with (h/B) is represented in Figure (11) and Figure (12). Adequate agreement results were noticed during comparing LEA to FEA with percentage 9.32 % as maximum for soil (1), 16.6% for soil (2) (Figure (12)).

Figure (13) illustrates the relations between I_f and h/B using the novel LEA ranged from 1 for equal side embedment to 2.866 as maximum for unequal side at h/B=2.0, and ranged from 1.355 to 2.866 for h/B (0.50 to 2.0) at different soil friction angles (30°, 33°, 36°). However Figure (13) indicated that I_f was proportional to h/B and soil friction angle, the effect of the increase in width of footing was marginal.

Figure (14) shows relations between partial shear failure factors (PSFF) and live load width ratio (LL/B). PSFF ranged from 0.522 to 0.255 for LL/B (0.0 to 10.0) at gravity wall width (4.0, 8.0) m and h/B (1.0 to 2.0). Figure (14) illustrates that PSFF is inversely proportional with LL/B.

Despite the inverse proportionality of PSFF with h/B, the wall width was insignificant, (Figure (15)). PSFF ranged from (0.675 to 0.411) for h/B (0.5 to 2.0) at soil friction angles of (30°, 33°, 36°) and gravity wall width (4.0, 8.0 m) (Figure (15)).
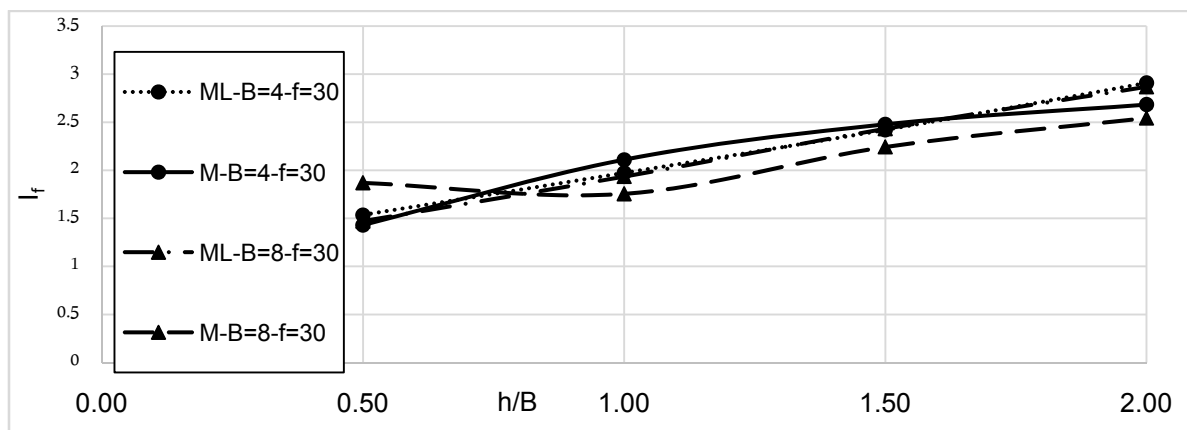

Figure (11) Comparison between LEA to FEA in calculating the improvement factor of the bearing capacity (I_f) for soil (1)
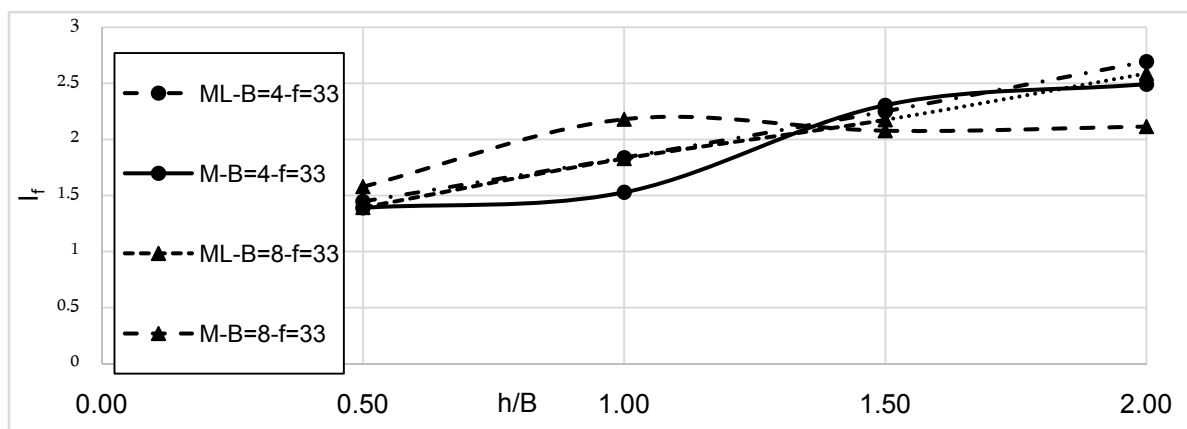

Figure (12) Comparison between LEA to FEA in calculating the improvement factor of the bearing capacity (I_f) for soil (2)
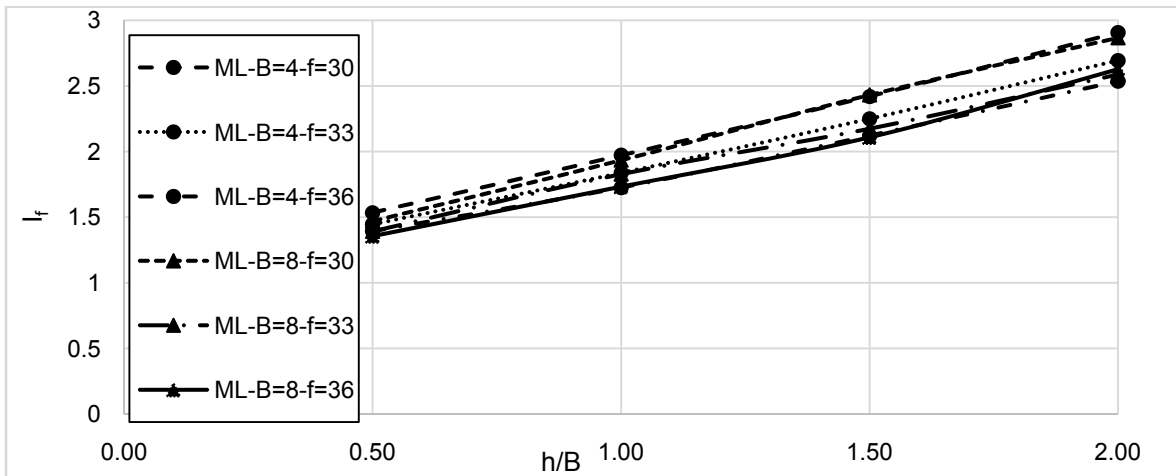
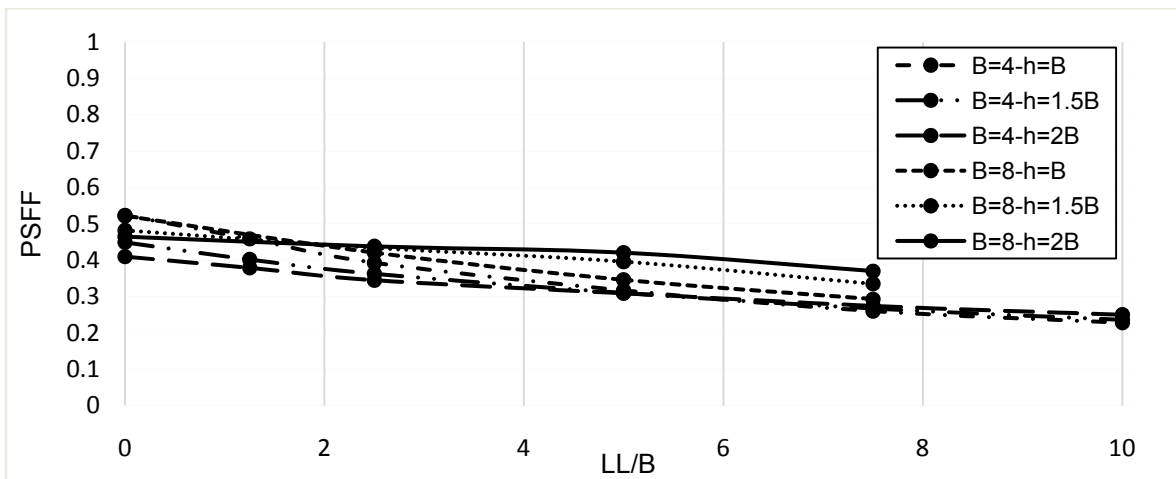**Figure (13) Improvement factor of bearing capacity using LEA (I_f)**

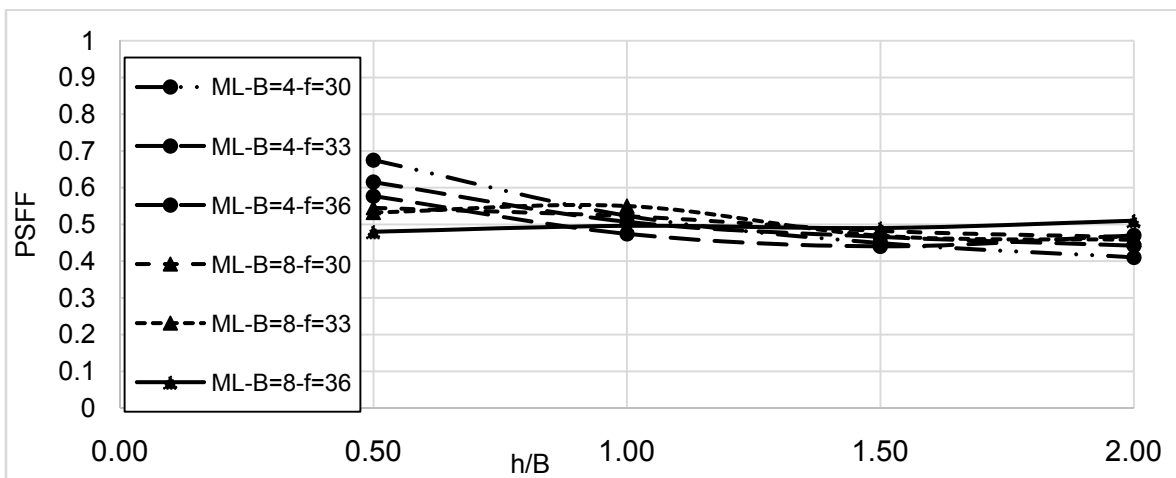**Figure (14) Variation of Partial shear failure factors (PSFF) with (LL/B)**

Figure (15) Variation of partial shear failure factors (PSFF) with (h/B)

Conclusion

- The novel limit equilibrium approach (LEA) has been studied, examined and verified successfully to obtain the improvement factor (I_f) of bearing capacity under shallow foundations and gravity walls for sandy soil with different friction angles.
- New semi-infinite surface load equation is integrated to facilitate the novel LEA.
- Over fifty finite element models have been built to be compared with the novel LEA for gravity walls.
- The improvement factor (I_f) diversity is proportional to h/B and soil friction angle, but the effect of increase in width of footing was marginal.
- The partial shear failure factor (PSFF) is inversely proportional to LL/B and h/B, but the wall width has minor significant effect.
- (I_f) ranged from 1 for equal side embedment to a maximum of 2.866 for unequal side at h/B=2.0 and ranged from 1.355 to 2.866 for h/B (0.50 to 2.0).
- The partial shear failure factor (PSFF) ranged from 0.522 to 0.255 for live load to width (LL/B) from 0.0 to 10.0 and ranged from 0.675 to 0.411 for h/B from 0.5 to 2.0.
- Future studies will be done for limit equilibrium approach applied on sandy soils with cohesion and stratified soils under gravity walls with different embedment sides.
- The new approach needs to be tested for inclined backfill embedment on bearing capacity improvement factor under gravity walls.
- Comparing the novel LEA with FEA using different material models, such as modified Mohr-Coulomb, the hardening and Drucker-Prager models.

REFERENCES

1. Vesic, A.S. (1973), "Analysis of ultimate loads of shallow foundations", J. of Soil Mech., Vol. 99(1), pp. 45-73.
2. Terzaghi, K. (1943), "Theoretical soil mechanics". Wiley, New York.
3. G. Meyerhof, G. (1951), "The Ultimate Bearing Capacity of Foudations", Vol. 2, pp. 301-332.
4. Burd H, F.S. (1997), "Bearing capacity of plane strain footings on layered", Canadian Geotechnical Journal 34: 241-253., pp. 34: 241-253.
5. DV, G. (1989), "Computation of collapse loads in geomechanics by finite", Ingenieur- Archiv pp. 59: 237- 244.
6. Jaeger JC, C.N. (1979),"Fundamentals of Rock Mechanics", London.
7. Mohr, O. (1900), "Welche Umsta¨nde bedingen die Elastizita¨tsgrenze undden Bruch eines Materials? Zeit des Ver Deut", pp. Ing 44:1524–1530.
8. CA, C. (1776), "Sur une application des regles maximis etminimis a quelques problems de statique, relatives a l'architecture", pp. 7:343–382.
9. Paul, B. (1968), "Generalized pyramidal fracture and yield criteria. Int JSolids Struct", pp. 4:175–196.
10. Meyer JP, L.J. (2012), "Linear failure criteria with three principalstresses", Int J Rock Mech Min Sci,Submitted.
11. BOUSSINESQ, J. (1883),"pplication des Potentials à L'Etude de L'Equilibre et du Mouvement des Solides Elastiques", Paris: Gauthier-Villars.
12. Prandtl, L. (1921), "Hauptaufsätze: Über die Eindringungsfestigkeit (Härte) plastischer Baustoffe und die Festigkeit von Schneiden", ZAMM - Journal of

Applied Mathematics and Mechanics / Zeitschrift für Angewandte Mathematik und Mechanik, Vol. 1 pp. 15-20.